Diminishing Interfacial Effects with Decreasing Nanoparticle Size in Polymer-Nanoparticle Composites

Hamed Emamy,[1] Sanat K. Kumar,[2,*] and Francis W. Starr[1,†]
[1]Department of Physics, Wesleyan University, Middletown, Connecticut 06459, USA
[2]Department of Chemical Engineering, Columbia University, New York, New York 10027, USA

(Received 21 June 2018; revised manuscript received 4 September 2018; published 13 November 2018)

Using molecular simulations on model polymer nanocomposites at fixed filler loading, we show that interfacial polymer dynamics are affected less with decreasing nanoparticle (NP) size. However, the glass transition temperature T_g changes substantially more for an extremely small NP. The reason for this apparent contradiction is that the mean NP spacing decreases with decreasing particle size. Thus, all polymers are effectively interfacial for sufficiently small NPs, resulting in relatively large T_g shifts, even though the interfacial effects are smaller. For larger NPs, interfacial relaxations are substantially slower than the matrix for favorable NP-polymer interactions. The minority "bound" polymer dynamically decouples from the polymer matrix, and we only find small changes in T_g relative to that of the bulk polymer for large NPs. These results are used to organize a large body of relevant experimental data, and we propose an apparent universal dependence on the ratio of the face-to-face distance between the NPs and the chain radius of gyration.

DOI: 10.1103/PhysRevLett.121.207801

Adding nanoparticles (NPs) to polymers is known to substantially alter mechanical, electrical, and optical properties [1–8], especially relative to traditional composites with micron scale additives [9–11]. Since these property improvements are driven by the NP surface-to-volume ratio, it is expected that NP size plays a central role in this context. Previous theories suggest that good NP dispersion, which is sometimes desirable [12–15], requires moderately favorable polymer-NP interactions. Even here a bound polymer layer, with relaxation times that are orders of magnitude slower than the surrounding bulklike polymer matrix [16–19], naturally forms. Long polymer chains that make multiple contacts with a surface can make the polymer adsorption effectively irreversible. While the number of contacts is proportional to $\sqrt{N}$ for chains of length N at a flat surface [20], it is smaller for more curved surfaces; thus, we expect that the temporal persistence of the bound layer should become weaker for smaller NPs. However, as we go to smaller NPs, the fraction of polymer chains interacting with a surface increases. The interplay between these two facts is an unresolved question that we shall focus on in this Letter.

Many experiments report little or no change of T_g for strongly interacting NPs with diameter $\gtrsim 10$ nm. Simulations suggest that a bound interfacial layer dynamically decouples from the surrounding polymer matrix in these situations [21]; since the matrix polymer dominates the observed behavior, there is relatively little observed change in T_g. In contrast, for small NPs (≈ 1 nm), experiments imply that there are large T_g shifts [22]. How NP size effects manifest themselves on dynamic phenomena such as the glass transition temperature T_g is then the second focus of the current Letter.

Using molecular dynamics simulations, we find that the effects of NPs on interfacial relaxation diminish with decreasing NP size (at fixed loading). However, the decreasing NP size leads to an increase in the fraction of interfacial polymer. Consequently, for small enough NPs, the polymer chains are effectively all interfacial. In this limit, the previous simulation results for larger NPs, which showed a decoupling of interfacial dynamics from that of the matrix, does not apply. This effect makes the T_g of the composite more sensitive to NP interaction strength for smaller NP sizes. This finding helps to explain the recent experimental work by Sokolov and co-workers [22], who observe substantial effects on T_g for small NPs.

Our findings are based on simulations of an ideal, uniform dispersion of NPs within a polymer matrix (earlier works provide more details [21,23]). The Kremer-Grest bead-spring model is used [24], with each chain comprised of 20 monomers of diameter σ. Nonbonded monomers interact via the Lennard-Jones (LJ) potential truncated and shifted beyond $r_c = 2.5\sigma$. Bonded monomers are linked by a finitely extensible nonlinear elastic potential. A collection of beads (identical to the monomers of polymer chains) are linked to form an icosahedral NP with specified size. A single NP is held fixed at the center of the simulation box surrounded by polymer chains with a NP filling fraction $\phi = 0.042$; given the periodic boundary conditions, this corresponds to ideal dispersion of NPs. Since the particle does not move in the simulation, the role of particle motion is not explored. We will focus on this topic in future work.

We study three different NP sizes that consist of 356, 104, or 12 beads, which correspond to an icosahedron with edge length $a = 6.6\sigma$, 4.4σ, or 2.1σ, respectively. This size can be converted to the diameter of an inscribed sphere following $d=(\sqrt{3}/6)(3+\sqrt{5})a$, resulting in $d = 10.0\sigma$, 6.6σ, and 3.3σ, respectively. To model the interaction between the NPs and polymers, we use an attractive LJ interaction, also truncated and shifted with $r_c = 2.5\sigma$. We systematically vary the polymer-NP interaction strength over $0.1 \leq \varepsilon \leq 3.0$, where ε is defined relative to the polymer-polymer interactions. Simulations are performed in an *NVT* ensemble along an isobaric path at pressure $P = 0.1$ for temperatures ranging from 0.40 to 0.80, in units of polymer-polymer interactions.

We first address how the NP size affects segmental relaxation and glass formation and the formation of a bound layer near the NP surface using the self-intermediate scattering function

$$F_{\text{self}}(q,t) = \frac{1}{N}\left\langle \sum_{j=0}^{N} e^{i\mathbf{q}\cdot[\mathbf{r}_j(t)-\mathbf{r}_j(0)]} \right\rangle, \quad (1)$$

where $r_j(t)$ is the position of monomer j at time t, and q is the wave vector. Following convention, we present results for $q_0 \approx 7$, the location of the primary peak in the monomer structure factor.

We quantify the spatial gradient of relaxation by calculating Eq. (1) conditioned on the radial distance r of a monomer from the NP at the time origin. Since monomers typically move only a fraction of a diameter over the relaxation time of $F_{\text{self}}(q,t)$, it does not matter whether we condition the position based on its starting value or the position after one relaxation time. As shown in Fig. 1 and previously [21], the relaxation near the surface is qualitatively different for weak versus strong polymer-NP interactions; namely, relaxation is enhanced near a weakly interacting substrate and slowed (by several orders of magnitude) at the strongly interacting substrate. For large NP diameter at this filling fraction, the layers furthest from the NP interface approach the behavior of a pure polymer melt at the same thermodynamic conditions.

$F_s(q_0,t,r)$ at a distance r from the NP follows a two-step relaxation

$$F_{\text{self}}(q,t,r) = [1-A(r)]e^{-(t/\tau_s)^{3/2}} + A(r)e^{[-t/\tau_\alpha(r)]^{\beta(r)}}, \quad (2)$$

where the first term is a vibrational relaxation and the second term represents the primary or α relaxation. The vibrational relaxation time is essentially independent of T, NP size, and ε, and we fix $\tau_s = 0.29$. The $t^{(3/2)}$ dependence corresponds to a Gaussian approximation to $F_s(q,t)$ with displacements that are intermediate between ballistic and Brownian motion [25]. The α-relaxation time $\tau_\alpha(r)$ as a function of distance $(r-d/2)$ from the NP surface is shown in Fig. 1(a) for two different interaction strengths,

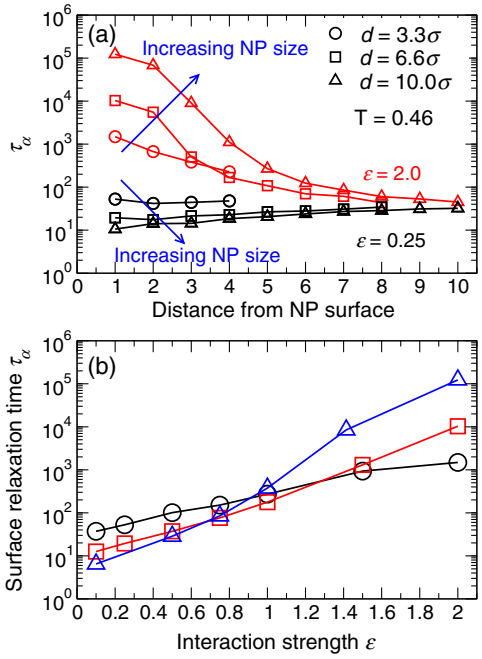

FIG. 1. (a) The monomer relaxation time as a function of distance from the NP surface for different NP sizes determined by fitting $F_{\text{self}}(q,t,r)$ using Eq. (2). For a weak NP interaction strength $\epsilon = 0.25$ (black lines), the monomer relaxation is enhanced approaching the NP surface. For a strong NP interaction strength $\epsilon = 2.0$ (red lines), the monomer relaxation is significantly slowed approaching the NP surface. (b) The relaxation time nearest to the NP surface as a function of interaction strength for different NP sizes. The data show that the effect of interactions on surface relaxation diminishes as NP size decreases.

$\varepsilon = 2.0$ (strong interaction) and $\varepsilon = 0.25$ (weak interaction), respectively, for all NP sizes studied at a temperature $T = 0.46$, above, but approaching T_g. ($T_g \approx 0.41$ for the bulk polymer at these conditions.) As expected, for $\varepsilon = 2.0$, the relaxation time increases near the NP interface, while the opposite behavior occurs for $\varepsilon = 0.25$. The important observation is that the change in the relaxation time relative to the pure polymer (whether it is increased or decreased) is substantially *smaller* for smaller NP size. For example, for the largest NP ($d = 10.0\sigma$) with $\varepsilon = 2.0$, the relaxation time near the interface is roughly 2 orders of magnitude larger than the smallest NP ($d = 3.3\sigma$), and the separation of these scales only grows with decreasing temperature. The effect of NP size on relaxation is less pronounced for $\varepsilon = 0.25$ [Fig. 1(b)].

The spatial variation of the dynamics accessible by simulations cannot be measured by most experiments. However, when the relaxation time of the interfacial layer becomes significantly larger than that of the polymer matrix, earlier work has shown that the overall relaxation function does indicate a distinct relaxation process of the interfacial layer, i.e., the bound polymer [26]. The dependence of the gradient of relaxation on NP size suggests that the effects of bound polymer should be diminished for

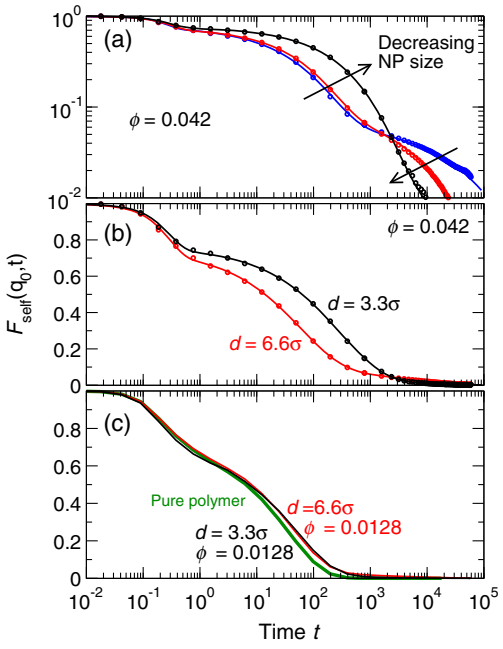

FIG. 2. (a) The intermediate scattering function for systems with different NP sizes at an identical NP concentration ($\phi = 0.042$). The primary and bound relaxation times show opposite dependences on particle size; specifically, the bound layer relaxation time decreases as the NP size decreases. For the smallest NP size ($d = 3.3\sigma$), this bound layer does not affect the T_g. (b) $F_{\rm self}(q,t)$ for particle sizes $d = 6.6\sigma$ and $d = 3.3\sigma$ and NP concentration $\phi = 0.042$ [same data as (a), but with a linear scale on the ordinal axis]. As a result of interfacial layer overlap, the primary relaxation time of the $d = 3.3\sigma$ system is significantly larger than that of the $d = 6.6\sigma$ system. (c) $F_{\rm self}(q,t)$ of the pure polymer and the composites at small NP concentration; for small ϕ, the interfacial layers do not overlap for any case so that the effect of NP size on the relaxation time is less significant.

smaller NPs, a phenomenon we now consider. The intermediate scattering function $F(q_0,t)$ for the system as a whole for different NP sizes is shown in Fig. 2 for a reference $T = 0.46$ and $\varepsilon = 2.0$. For $d = 10.0\sigma$ and $d = 6.6\sigma$, the bound polymer contribution to $F(q_0,t)$ is apparent from the additional relaxation process at large t, most readily seen on a double-logarithmic scale [Fig. 2(a)]. Such a bound polymer is only apparent when the polymer-NP interaction strength follows $\varepsilon \gtrsim 1$. For the smallest NP size ($d = 3.3\sigma$), the distinction between the primary and the secondary (bound) relaxation is very weak. This is because the separation between a NP and its periodic images is small enough that the interfacial zones of NP overlap, so that there is effectively no bulklike matrix relaxation. For systems with a distinct bound relaxation, $F(q_0,t)$ can only be described by including an additional relaxation process [21,27,28],

$$F_{\rm self}(q,t) = (1-A)e^{-(t/\tau_s)^{3/2}} + (A-A_b)e^{-(t/\tau_\alpha)^{\beta}} + A_b e^{-(t/\tau_b)^{\beta_b}}. \quad (3)$$

We thus extract the fit parameters A (the amplitude of the vibrational relaxation), A_b (the bound monomer fraction), τ_α (the primary relaxation), τ_b (the bound interfacial monomer relaxation), and the associated stretching exponents β and β_b. τ_b decreases as the NP size decreases, as expected from the relaxation near the NP surface (Fig. 1). In other words, smaller NPs are less effective at creating a surface layer with substantially slowed-down dynamics.

To separate the influence of the overlap of interfacial layers on adjacent NPs from the effect of NP size on the interfacial layer, we performed additional simulations at very low NP concentrations $\phi = 0.0128$ for composites with NP sizes $d = 3.3$ and $d = 6.6$. At the higher concentration discussed above ($\phi = 0.042$), the system with the smallest NP ($d = 3.3\sigma$) shows a significantly slower relaxation of $F(q,t)$ than the system with the larger NP ($d = 6.6\sigma$) [Fig. 2(b)]. In contrast, at the lower NP concentration, the difference between the $F(q,t)$ for different NP sizes is substantially diminished [Fig. 2(c)]. These results argue for the importance of the overlap of interfacial layers on adjacent NPs on the self-intermediate scattering function, an effect that is magnified for high concentrations of the smallest NPs.

To highlight the effects of changes in the bound layer relaxation time with NP size, we evaluate the dynamical T_g by the temperature at which the relaxation time reaches a value of 1000 in LJ units. The relaxation time is defined when $F(q_0,t) = 1/e$. Note that this value of τ is distinct from either τ_α or τ_b obtained from the three-scale fit [Eq. (3)]. The resulting T_g obtained from both the overall relaxation time τ and the matrix relaxation time τ_α are plotted as a function of interaction strength for different NP size. Figure 3 shows that the T_g of the overall composite is more strongly affected at large ε for the smaller NP size than for the larger NP size, despite the fact that τ_b is smaller for the smaller NP; this is a consequence of the larger surface-to-volume ratio for the same NP concentration when NPs are smaller. For the overall T_g, a naive expectation is that the T_g increases linearly with the interaction strength. This holds only for the smallest NP where all polymers are essentially interfacial, but does not hold for larger NPs ($d = 10.0$ and $d = 6.6$) [Fig 3(b)]; for these larger NPs, the "cloaking" effect of the bound layer reduces the increase in T_g as the ε increases. This confirms our expectation that T_g should be more strongly affected when the interfacial zones overlap. This effect can also account for the enhanced effect on T_g for small NP size that has been observed experimentally [22]. Indeed, for the concentration shown here ($\phi \approx 0.05$), the scale of T_g changes is comparable to that seen experimentally.

Our results suggest a unified understanding of T_g changes in attractively interacting polymer nanocomposites. There are several relevant length scales to consider, namely, the mean face-to-face separation between NPs r, the length scale of interfacially dominated dynamics ξ (typically a few monomer diameters), and the chain radius

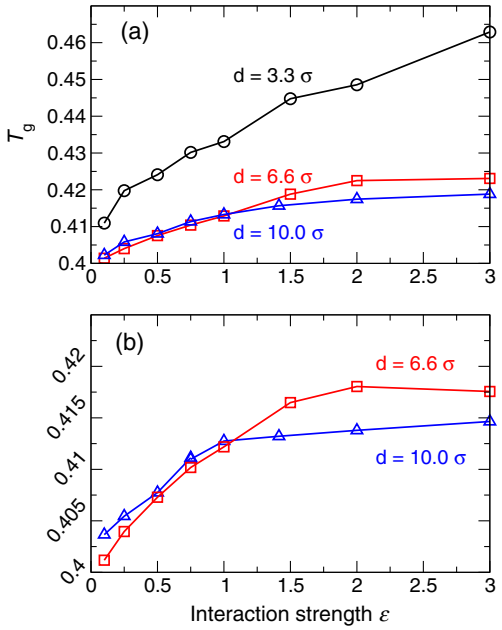

FIG. 3. (a) The glass transition temperature T_g for the *overall* composite for all NP sizes with identical NP concentration. The T_g changes are larger for smaller NPs. For the smallest NP ($d = 3.3$), T_g increases roughly linearly with ε, qualitatively different from that for the larger NP; this is due to the overlap of the interfacial zones for the smallest NP. (b) T_g for the polymer matrix for different NP sizes with identical NP concentration; data for the NP size $d = 3.3$ are not included, since all polymers are interfacial for this case. The smaller NP has a larger effect on matrix T_g.

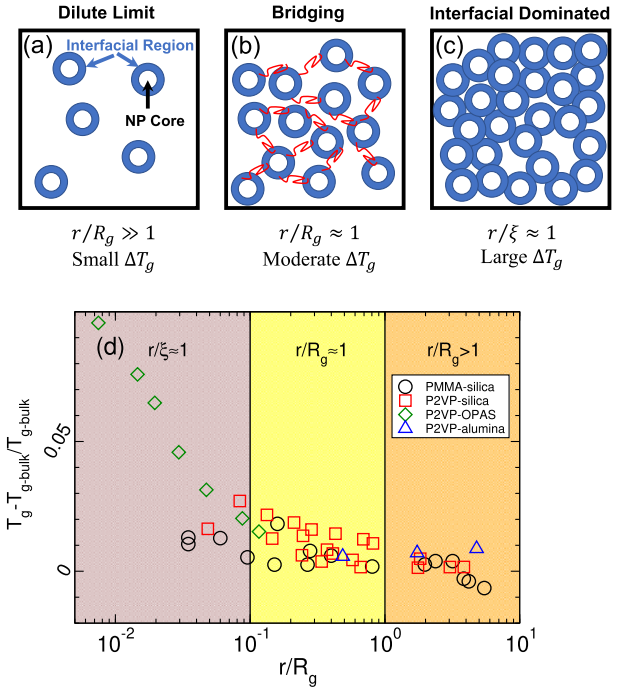

FIG. 4. Schematics of the different regimes for interfacial effects of the NP. (a) The dilute regime, where the dynamics of interfacial polymer decouples from that of the polymer matrix when polymer-NP interactions exceed those of the matrix, leading to very little T_g change. (b) The "bridging regime," where the separation of the NPs allows the interfacial chains to bridge. The bridging of the interfacial polymers leads to a higher change in T_g than in the dilute regime. (c) The interfacially dominated regime, where the concentration of NPs is high enough that interfacial zones overlap. In this regime, the T_g has the largest change compared to the pure melt. The value of r/R_g for $d = 3.3\sigma$, $d = 6.6\sigma$, and $d = 10.0\sigma$ is $r/R_g = 3.3/2.16 = 1.52$, $r/R_g = 6.6/2.16 = 3.05$, and $r/R_g = 10.0/2.16 = 4.63$, respectively. (d) The normalized change of T_g as a function of r/R_g. The systems shown are composites of PMMA-silica (black circles), poly-2-vinyl pyridine (P2VP)-silica (red squares), OPAS-silica (green diamonds), and P2VP-alumina (blue triangles). These data are gathered from Refs. [16,18,19,22,29,30]. To estimate the mean face-to-face separation r between NPs, we use the expression $r/d = (\phi_{\max}/\phi)^{1/3} - 1$ [31], where $\phi_{\max}$ is the maximum filling fraction ($\phi_{\max} \approx 0.7$), d is the NP diameter, and ϕ is the NP filling fraction.

of gyration R_g (typically $> \xi$). Obviously, the effects will be most pronounced when the interfacial zones on adjacent NPs overlap ($r/\xi \lesssim 1$), but we anticipate that interfacial effects also play a significant role at larger separations through chain bridging effects ($r/R_g \lesssim 1$). Because we examined relatively short chains here ($1.5 \lesssim r/R_g \lesssim 5$), such bridging effects are not apparent in our simulations. Figure 4 schematically shows that the most interesting case arises for large ε. If the NP concentration is low enough that $r/R_g \gg 1$, the dynamics of the interfacial polymer decouples from the polymer matrix. This decoupling serves to "cloak" the NP and results in the unexpected finding of little or no increase in the measured T_g for strong ε [21]. The concentration at which these interfacial regions will start to affect each other (i.e., when $r/R_g \lesssim 1$) will be NP size dependent, since, at a given concentration, the NP separation is smaller for smaller diameter NPs. In other words, the critical concentration where interfacial effects will begin to dominate T_g changes decreases for smaller NPs. In addition, with smaller separation r, confinement effects will be more pronounced. Both of these effects tend to lead to larger T_g shifts for smaller NPs.

To support these arguments, Fig. 4(d) shows experimental data for the normalized change in T_g of several polymer-nanoparticle composites for a range of r/R_g values. For the largest r/R_g, there is only a small change in the T_g, consistent with our predictions for the behavior of the dilute regime [Fig. 4(a)]. When $r/R_g \lesssim 1$, the experimental results show larger increases in the normalized T_g. Finally, even smaller r/R_g values lead to large increases in T_g, as expected. There are a few exceptions to these apparently general trends that are worth emphasizing. Recent work by Fakhraai and coworkers [32] found that, for densely packed, but random NP assemblies, T_g shifts were larger for longer chain length polymers, a finding that is consistent with our

assertion that the relevant control parameter is r/R_g. However, the precise value of r/R_g is hard to estimate here since the NPs are in contact with each other. The increases found for the normalized $\Delta T_g \approx 0.075$ [based on Fig. 4(d)] corresponds to $r/R_g \approx 0.015$. Whether this estimate is reasonable remains to be verified. Rittigstein and Torkelson's [33] measurements of the ΔT_g for alumina-P2VP are significantly higher than those shown in Fig. 4(d). We do not know the exact reason for this deviation, but conjecture it may be due to the difference in the experimental method that is used to measure T_g. Nonetheless, in broad strokes, the experimental data are consistent with our simulations in that they suggest that the relevant parameter here is r/R_g and that the normal shifts in T_g increase monotonically (and apparently in a quasiuniversal) manner with decreasing r/R_g.

We thank J. F. Douglas for helpful discussions. Computer time was provided by Wesleyan University. This work was supported in part by NIST Grant No. 70NANB15H282. Financial support for this research was provided by the NSF through Grant No. DMR-1709061.

*sk2794@columbia.edu
†fstarr@wesleyan.edu

[1] J. H. Koo, in *Fundamentals, Properties, and Applications of Polymer Nanocomposites* (Cambridge University Press, Cambridge, England, 2016), pp. 550–565.
[2] R. Gangopadhyay and A. De, Chem. Mater. **12**, 608 (2000).
[3] A. C. Balazs, T. Emrick, and T. P. Russell, Science **314**, 1107 (2006).
[4] G. Schmidt and M. M. Malwitz, Curr. Opin. Colloid Interface Sci. **8**, 103 (2003).
[5] J. F. Moll, P. Akcora, A. Rungta, S. Gong, R. H. Colby, B. C. Benicewicz, and S. K. Kumar, Macromolecules **44**, 7473 (2011).
[6] J. Jordan, K. I. Jacob, R. Tannenbaum, M. A. Sharaf, and I. Jasiuk, Mater. Sci. Eng. A **393**, 1 (2005).
[7] J. Jancar, J. Douglas, F. W. Starr, S. Kumar, P. Cassagnau, A. Lesser, S. S. Sternstein, and M. Buehler, Polymer **51**, 3321 (2010).
[8] W. Caseri, Macromol. Rapid Commun. **21**, 705 (2000).
[9] K. Sanada, Y. Tada, and Y. Shindo, Composites A **40**, 724 (2009).
[10] J. Cho, M. Joshi, and C. Sun, Compos. Sci. Technol. **66**, 1941 (2006).
[11] W. Gacitua, A. Ballerini, and J. Zhang, Maderas Cienc. Tecnol. **7**, 159 (2005).
[12] F. W. Starr, J. F. Douglas, and S. C. Glotzer, J. Chem. Phys. **119**, 1777 (2003).
[13] P.-C. Ma, N. A. Siddiqui, G. Marom, and J.-K. Kim, Composites A **41**, 1345 (2010).
[14] T. Kashiwagi, F. Du, K. I. Winey, K. M. Groth, J. R. Shields, S. P. Bellayer, H. Kim, and J. F. Douglas, Polymer **46**, 471 (2005).
[15] J. Fu and H. E. Naguib, Journal of Cellular Plastics **42**, 325 (2006).
[16] P. Rittigstein, R. D. Priestley, L. J. Broadbelt, and J. M. Torkelson, Nat. Mater. **6**, 278 (2007).
[17] A. P. Holt, P. J. Griffin, V. Bocharova, A. L. Agapov, A. E. Imel, M. D. Dadmun, J. R. Sangoro, and A. P. Sokolov, Macromolecules **47**, 1837 (2014).
[18] A. P. Holt, J. R. Sangoro, Y. Wang, A. L. Agapov, and A. P. Sokolov, Macromolecules **46**, 4168 (2013).
[19] S. E. Harton, S. K. Kumar, H. Yang, T. Koga, K. Hicks, E. Lee, J. Mijovic, M. Liu, R. S. Vallery, and D. W. Gidley, Macromolecules **43**, 3415 (2010).
[20] A. Silberberg, J. Colloid Interface Sci. **90**, 86 (1982).
[21] F. W. Starr, J. F. Douglas, D. Meng, and S. K. Kumar, ACS Nano **10**, 10960 (2016).
[22] S. Cheng, S.-J. Xie, J.-M. Y. Carrillo, B. Carroll, H. Martin, P.-F. Cao, M. D. Dadmun, B. G. Sumpter, V. N. Novikov, K. S. Schweizer, and A. P. Sokolov, ACS Nano **11**, 752 (2017).
[23] F. W. Starr, T. B. Schroder, and S. C. Glotzer, Macromolecules **35**, 4481 (2002).
[24] G. S. Grest and K. Kremer, Phys. Rev. A **33**, 3628 (1986).
[25] D. S. Simmons and J. F. Douglas, Soft Matter **7**, 11010 (2011).
[26] Note that an extra bound layer relaxation does not manifest itself explicitly when we consider $F_{\mathrm{self}}(q,t,r)$ at each r—we see only two-step relaxation behavior at each r. It is the large gradient in this local relaxation that yields distinct relaxation processes in the total relaxation function.
[27] M. Solar, K. Binder, and W. Paul, J. Chem. Phys. **146**, 203308 (2017).
[28] L. Yelash, P. Virnau, K. Binder, and W. Paul, Europhys. Lett. **98**, 28006 (2012).
[29] J. Moll and S. K. Kumar, Macromolecules **45**, 1131 (2012).
[30] Z. Wang, Z. Lu, C. Mahoney, J. Yan, R. Ferebee, D. Luo, K. Matyjaszewski, and M. R. Bockstaller, ACS Appl. Mater. Interfaces **9**, 7515 (2017).
[31] T. Hao and R. E. Riman, J. Colloid Interface Sci. **297**, 374 (2006).
[32] J. L. Hor, H. Wang, Z. Fakhraai, and D. Lee, Soft Matter **14**, 2438 (2018).
[33] P. Rittigstein and J. M. Torkelson, J. Polym. Sci. B Polym. Phys. **44**, 2935 (2006).